

INTERFEROMETRIC FIBER OPTIC TEMPERATURE SENSOR

*A Thesis Submitted
in Partial Fulfilment of the Requirements
for the Degree of*

MASTER OF TECHNOLOGY

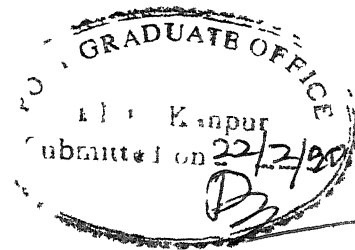
1990

by

S S GATTANI

to the

DEPARTMENT OF ELECTRICAL ENGINEERING
INDIAN INSTITUTE OF TECHNOLOGY KANPUR
FEBRUARY, 1990



CERTIFICATE

It is certified that the work contained in the thesis entitled "Interferometric Fiber Optic Temperature Sensor" by Mr. S.S. GATTANI, has been carried out under our supervision and that the work has not been submitted elsewhere for a degree.

Pradip Sircar
Dr. P. Sircar

Asstt Professor
Dept. of Electrical Engg.
I.I.T. Kanpur

R. Sharan
Dr. R Sharan

Professor
Dept. of Elect Engg.
I.I.T. Kanpur

9 APR 1990

CENTRAL LIBRARY
KAMPUR

Acc No A107305

EE-1990-M-GAT-INT

ACKNOWLEDGEMENTS

I wish to thank my guides Dr. R. SHARAN and Dr P. SIRCAR for their encouragement given throughout this work. I sincerely grateful to Dr. K.K. Sharma of Physics Deptt. and Dr. J. Narain of Electrical Engg. Deptt for all their help. Mr. Sandeep Agrawal of EE Deptt. deserves special thanks for the fruitful discussion and suggestions

Finally I would like to extend my thanks to all my colleagues in particular K Murlī Krishna, K. Shrikant and U.N. Reddy.

S.S. Gattani

ABSTRACT

Interferometric fiber optic sensors using single mode fibers are described. The choice of Mach-Zehnder interferometer is explained as well as its application for temperature measurement. Temperature can be monitored by detecting the fringe movement generated due to changes in pathlength in the sensing arm of Mach-Zehnder Interferometer.

A Mach-Zehnder interferometer has been setup and fringes have been observed on the screen. A simple detection scheme demonstrates the shift in fringe pattern with change in temperature. Different problems in setting up the Mach-Zehnder-Interferometer are described. Finally advanced phase detection techniques are reviewed as well as guidelines for future work and potential market areas are discussed.

CONTENTS

	Page No
CHAPTER 1 INTRODUCTION	1
1.1 . Fiber optic sensor development	
1.2 Scope of work	
1.3 Future trends in interferometric sensor	
CHAPTER 2 THEORY OF INTERFEROMETRIC SENSORS	5
2 1 Discovery of interference	
2 1.1 Conditions for interference	
2.1.2 Double-slit interference	
2.1.3 . Two-beam interference	
2 1.4 Mach-Zehnder interferometer	
2.2 : Principle of operation of fiber optic temperature sensor based on M-Z-I	
2 2 1 : Principle of operation	
2 2 2 : Analysis	
2 3 : Difficulties in M-Z-I sensor system	
2 3.1 . Optical alignment for source to fiber coupling	
2.3.2 : Propagation of higher order modes and attenuation consideration	

2.3.3	Beam splitter microphonics	
2.3.4	: Light source selection and associated problems	
2.3.5	: Modal noise	
2.3.6	: Effect of other physical variables	
2.4	: Detection system	
2.4.1	: Photo detector	
2.4.2	: Preamplifier and amplifier	
CHAPTER 3	SIGNAL RECOVERY TECHNIQUES FOR FIBER OPTIC INTERFEROMETRIC SENSORS	29
3.1	. Introduction	
3.1.1	: Passive homodyne (HOM)	
3.1.2	Phase tracking homodyne detection systems (PTDC & PTAC)	
3.1.3	: Heterodyne detection system (HET)	
3.1.4	Synthetic heterodyne detection system (SHET)	
3.2	. Interferometric sensor detection system tradeoff	
CHAPTER 4	EXPERIMENT AND RESULTS	42
4.1	. Experiment	
4.2	: Detection scheme	
4.2.1	: Circuit description	

4.3	Component specifications	
4.4	Results	
CHAPTER 5	DISCUSSION/MARKET AREAS & CONCLUSIONS	48
5.1	Technologies	
5.2	Market areas	
5.3	Conclusions	
REFERENCES		52

List of Figures

			Page No.
1	Fig 2.1	Double-slit interference	7
2.	Fig. 2.2	Two beam interference	7
3	Fig. 2.3	Mach-Zehnder Interferometer	10
4	Fig. 2.4	M-Z interferometer fiber optic temperature sensor	12
5	Fig 2.5	Geometry of source-fiber coupling errors	17
6	Fig. 2.6	Expanded beam connector	18
7.	Fig 2.7	LP modes propagation	20
8	Fig. 2.8	Detection system	26
9.	Fig. 3.1	Generalized fiber interferometer and detection system	30
10.	Fig. 3.2	PTDC detection system	30
11.	Fig. 3.3	Synthetic heterodyne (SHET) detection system	39
12.	Fig. 4.1	Photodetector circuit diagram	44
13.	Fig. 4.2	Fringe pattern	47
14.	Fig 5.1	Technology trend in optical fiber sensor	49

List of Tables

1.	Table I	Detection systems	32
2	Table II	Detection system tradeoff	41
3	Table III	Optical fiber sensor market	50

CHAPTER - I

INTRODUCTION

1.1 Fiber optic sensor development

Optical fiber sensor development has matured to the point where the impact of this new technology is now evident. Optical fiber sensors offer a number of advantages:

- increased sensitivity over existing techniques,
- geometric versatility in that fiber sensors can be configured in arbitrary shapes,
- a common technology base from which devices to sense various physical parameters (acoustic, magnetic, temperature, pressure etc.) can be constructed,
- dielectric construction so that it can be used in high voltage, electrically noisy, high temperature, corrosive or other extreme environments,
- compatibility with optical fiber telemetry technology.

Progress in demonstrating these advantages has been substantial in the past few years with over sixty different sensor types having been developed [1].

Fiber-optic sensors are categorized into amplitude or phase (i.e. interferometric) sensors. In the former case the physical parameters cause the fiber or some device attached to the

fiber to directly modulate the intensity of the light in the fiber. The advantages of intensity sensors are the simplicity of construction and compatibility with multimode fiber technology. In view of their simplicity the multimode fiber sensors should prove useful for threshold detection but they can not be relied upon to give amplitude information when the signal exceeds a certain threshold. Hence these are suited for the study of dynamic changes only.

The phase (i.e. interferometric) sensor, (whether for acoustic sensing, magnetic sensing, temperature sensing etc.) offers increased sensitivity over the existing technologies. These sensors use single mode fibers to configure a Mach-Zehnder interferometer in which the laser light from the sensing fiber is mixed with a stable reference to produce interference. Various phase detection techniques can be used to detect the change in phase caused due to the change in the pathlength of the optical fiber. Very minute change in either the length of the fiber or its refractive index leads to sufficient change in phase difference between two arms and hence the sensitivity of the sensor increases.

1.2 Scope of the work

The purpose of the present work is to establish and reproduce the above mentioned principle of Mach-Zehnder

interferometric sensor and to demonstrate the sensitivity of this sensor for the measurement of temperature and other physical parameters. The sensor system uses a cw He-Ne laser source and direct measurement of interference fringes using a simple detection scheme. Various intricacies of a M-Z interferometer and its optical components are discussed. The sensitivity of a M-Z-I sensor to temperature changes is demonstrated. Finally review of more advanced phase detection techniques is done and guide lines for future developmental work are discussed.

1.3 Future trends in interferometric sensor

Presently there is no commercial version of interferometric sensor available, though, there are a number of promising laboratory prototypes which have been demonstrated [7].

There are two major areas of activity as follows

The first is in taking the concepts which have been demonstrated in the laboratory into production engineering. To do this there are innumerable practical difficulties that have to be overcome, some of which are

- the technology is neither fully developed nor it is exploited
- practical problems remain in the area of new sources, detection scheme
- packaging
- optimized fiber coating.

interferometric sensor and to demonstrate the sensitivity of this sensor for the measurement of temperature and other physical parameters. The sensor system uses a cw He-Ne laser source and direct measurement of interference fringes using a simple detection scheme. Various intricacies of a M-Z interferometer and its optical components are discussed. The sensitivity of a M-Z-I sensor to temperature changes is demonstrated. Finally review of more advanced phase detection techniques is done and guide lines for future developmental work are discussed.

1.3 Future trends in interferometric sensor

Presently there is no commercial version of interferometric sensor available, though, there are a number of promising laboratory prototypes which have been demonstrated [7].

There are two major areas of activity as follows

The first is in taking the concepts which have been demonstrated in the laboratory into production engineering. To do this there are innumerable practical difficulties that have to be overcome, some of which are

- the technology is neither fully developed nor it is exploited
- practical problems remain in the area of new sources, detection scheme
- packaging
- optimized fiber coating.

The second major development lies in the research laboratory where there is considerable interest in a multiplexing system. By this method several sensors may be integrated simultaneously along a single linking fiber. All these systems rely upon a differential path to encode the location of each particular sensor. The path difference may be within the sensor itself (via static path encoding) or it may be in terms of the physical distance from the source to the receiver via the sensor element. In order to identify each of the sensors within the network, it is necessary to modulate the waveform applied to the network. The system imposes stringent conditions on the spectrum of the waveform introduced in the network. In this respect, interferometric sensors are more demanding than fiber-optic sensors based on the modulation of other optical parameters in that the coherent function must be maintained for all sensing elements. The experimental demonstrations that have been reported have achieved limited success. There is clearly considerable scope for further development [7].

CHAPTER - 2

THEORY OF INTERFEROMETRIC SENSORS

2.1 Discovery of Interference

The phenomenon of interference of light was first demonstrated by Thomas Young (1801) using double slit experiment [10]

2.1.1 Conditions for Interference

Interference between two beams occur under the following conditions

- (i) The two beams which interfere must originate from the same source of light, so that they are in same phase or have a constant phase difference
- (ii) The amplitude of the two interfering waves must be equal or nearly equal
- (iii) The source should be monochromatic.
- (iv) The two interfering beams should be propagating in the same direction, or in other words, the two interfering wavefronts must intersect at a very small angle
- (v) Lastly, the two interfering waves must be in the same state of polarization

2 Double-slit Interference

The double-slit experimental arrangement is as shown in fig.

In this experiment it was assumed that the slit width was comparable with the wavelength of the light and with the opaque plate separating the two slits. The interference pattern formed on the screen is characterized by a number of equally spaced interference maxima and minima.

For L sufficiently large, the optical path difference is

$$r_1 - r_2 = d \sin \theta \quad (2.1)$$

Intensity, I at a point P is proportional to the square of amplitude. Hence

$$I = 4A^2 \cos^2 \phi/2 \quad (2.2)$$

where ϕ is a phase difference.

In particular, the conditions for maximum and minimum intensity are respectively,

$$I = 4A^2 \quad \text{when } \phi = 2m\pi, \quad (2.3)$$

$$I = 0 \quad \text{when } \phi = (2m+1)\pi, \quad (2.4)$$

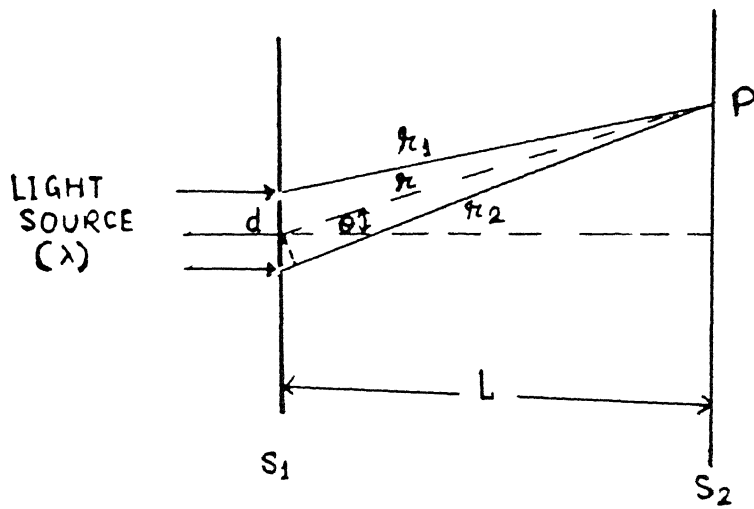


FIG 2 1
Double-slit interference

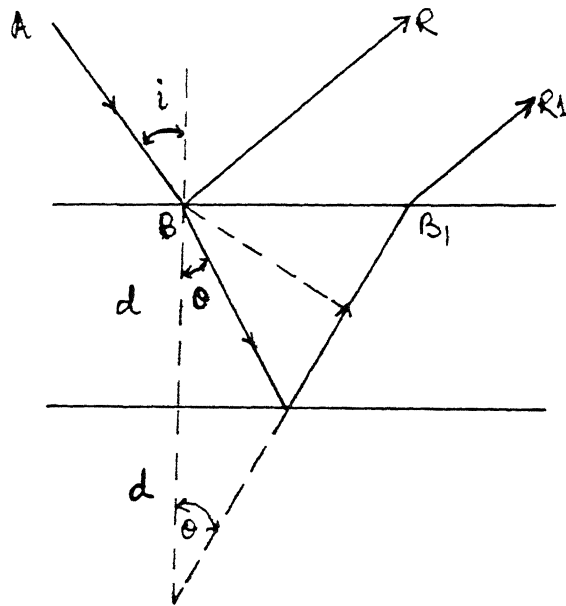


FIG 2 2
Two beam interference

where $m = 0, 1, 2, \dots$ etc.

2.1.3 Two-beam Interference

Two beam interference is obtained when a plane monochromatic light wave of wavelength λ is incident on the surface of a thin film. The two beams reflected by the upper and lower surface of the thin film interfere to give a pattern of maximum and minimum intensity as shown in fig. 2.2

The optical path difference is given by

$$OPD = 2d\mu \cos \theta \quad (2.5)$$

The phase difference due to OPD will be

$$\phi = \frac{2\pi}{\lambda} [\mu 2d \cos \theta] \quad (2.6)$$

where μ is the refractive index of the film.

The intensity is given by

$$I = 4A^2 \cos^2 \left[\frac{2\pi}{\lambda} \mu 2d \cos \theta \right] \quad (2.7)$$

For maximum and minimum intensity the conditions are

$$\begin{aligned}\phi &= 2m\pi && \text{for maximum} \\ &= (2m+1)\pi && \text{for minimum,}\end{aligned}$$

where $m = 0, 1, 2, \dots \text{etc}$

2.1.4 Mach-Zehnder Interferometer

The basic M-Z interferometer is shown in fig. 2.3. Light from the source is divided into two parts using a beam splitter. The two beams are reflected using mirrors and combined again using another beam splitter. If the pathlength travelled by the two beams is different, interference will take place and a stationary pattern results at the output [9].

2.2. Principle of operation of fiber optic temperature sensor based on M-Z-I

The above three examples satisfy the conditions described for obtaining interference. While the Young's experiment and two beam technique are the old examples of interference, M-Z-I is one of the many modern interferometric techniques. Other techniques are Fabry-Perot interferometer, Michelson interferometer etc. The design of the M-Z interferometer is the simplest in this class of techniques. Hence, it is often used at a laboratory

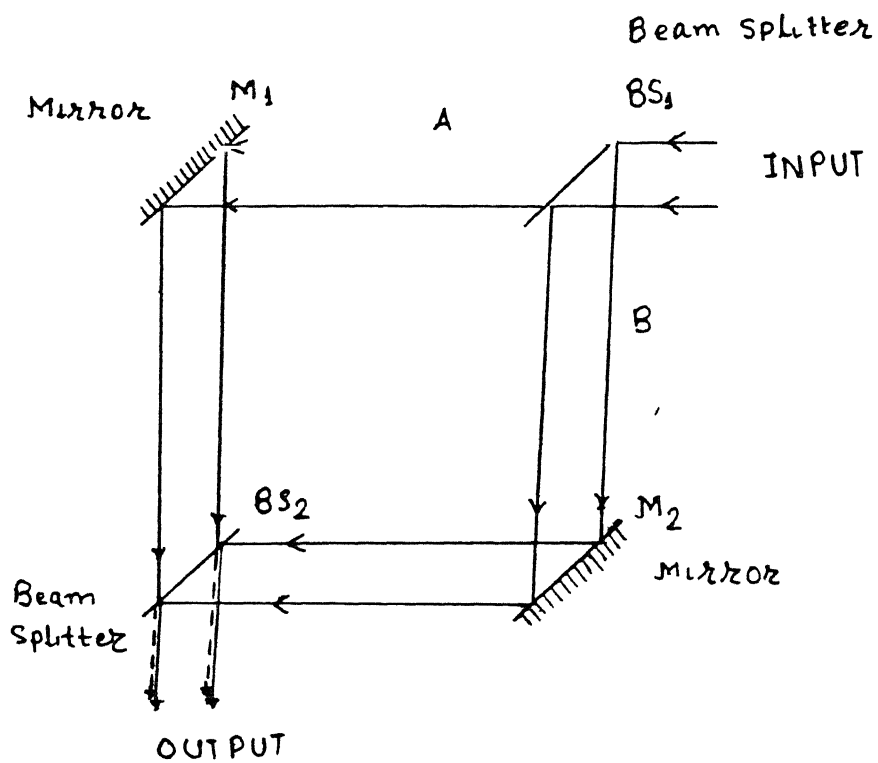


FIG 2 3

Mach-Zehnder interferometer

level. In more complex sensor systems, the latter techniques are used giving better sensitivities. However, these are extremely difficult to setup at a laboratory level. Hence in the present work, an M-Z interferometer is used to establish the fiber optic temperature sensor.

2.2.1 Principle of operation

An M-Z interferometer can be made using single mode optical fibers for the two arms as shown in fig 2.4. If the optical pathlengths of the two arms are nearly equal (to within the coherence length of the source), the light from the two fibers interfere to form a series of dark and bright fringes. A change in the relative phase of the light from one fiber with respect to the other is observed as a displacement of the fringe pattern. A phase difference of 2π radians causes a displacement of one fringe [4].

The pathlength of the light leaving the fiber can be changed either by changing its length and/or by changing its index of refraction. For optical fibers, both the length of the fiber as well as its index of refraction changes with temperature. These changes have been well studied for different fiber optic materials [1]. The sensing arm is subjected to the changing environment while the reference arm is maintained at constant

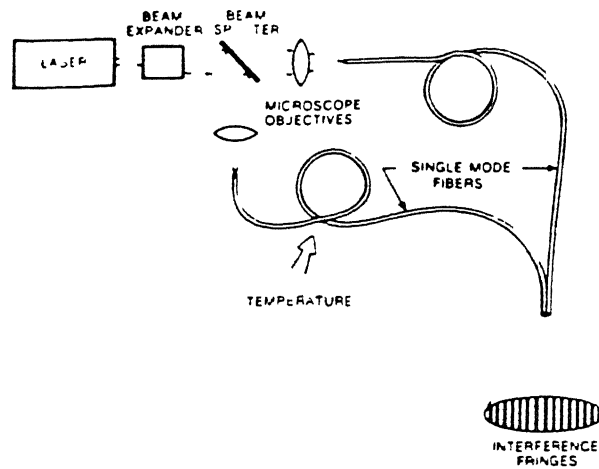


FIG 2 4

M-Z interferometer fiber optic sensor

temperature. Thus the difference in temperature gets reflected as a change of phase difference between the two fiber arms. This forms the basis of the M-Z-I temperature sensor.

2.2.2 Analysis

The basic quantity to be calculated is the optical phase change per unit fiber length per unit of the physical stimulus considered, i.e., $(\Delta\phi)/(SL)$, where

$\Delta\phi$ is the phase change in radians,

L is the fiber length, and

S is the stimulus such as pressure, temperature etc

(a) Temperature Sensitivity

A change in temperature of fiber, ΔT , changes the optical phase of the light going through it $\Delta\phi$ due to two effects

- (i) the change in fiber length due to thermal expansion or contraction,
- (ii) the temperature induced change in the index of refraction.

Since

$$\phi = \frac{nL2\pi}{\lambda}, \quad (2.8)$$

we can write

$$\frac{\Delta\phi}{\Delta TL} = \frac{2\pi}{\lambda} \left(\frac{n}{L} \frac{dL}{dT} + \frac{dn}{dT} \right) \quad (2.9)$$

where,

L = interaction length

$\frac{dn}{dT}$ = refractive index temperature coefficient

n = mean refractive index of core

λ = wavelength of laser source.

In equation 2.9, effects of fiber diameter changes are neglected since these are small.

Taking the case of He-Ne laser source and fused silica fiber and substituting various parameter values in equation 2.9, we get

$$\frac{1}{L} \frac{dL}{dT} = 5 \times 10^{-7} / ^\circ\text{C}$$

$$\frac{dn}{dT} = 10 \times 10^{-6} / ^\circ\text{C}$$

$$n = 1.456$$

$$\lambda = 0.6328 \times 10^{-6} \text{ m}$$

such that,

$$\frac{\Delta\phi}{\Delta T L} = 107 \text{ radians/}^{\circ}\text{C-m} \quad (2.10)$$

Stated differently, there is a fringe displacement of 170 fringes per $^{\circ}\text{C}$ per meter of fiber [4].

The values for thermal expansion coefficient and the temperature dependent refractive index can vary greatly for multicomponent glasses. Moreover $\frac{dn}{dT}$ itself is a function of temperature and wavelength. Therefore, the values of $\frac{\Delta\phi}{\Delta T L}$ could be quite different from that given in equation 2.10 for other glass compositions.

2.3 Difficulties in M-Z-I sensor system

There are many difficulties in component selection for M-Z-I sensors. Some of these are discussed below along with the errors introduced in the system. These errors pertain to optical alignment for source to fiber coupling, propagation of higher order modes in the fiber, optical feedback to the laser source, and various kinds of random noise phase shifts present in the system. All these difficulties in setting up the M-Z interferometer are discussed along with various design options.

2.3.1 Optical alignment for source to fiber coupling

The problem of optical power injection into the fiber is one of the most important in an optical fiber system. In fact a lot of power is lost in the coupling region between the source and the fiber. This is so because the beam width of the source is much larger than the diameter of the fiber core. Hence an additional optical element [e.g. a beam expander] has to be incorporated in the system. In practice, direct coupling conditions can rarely be achieved. It is important to analyse the launching efficiency of the beam expander as well as various coupling error parameters. There are three kinds of fundamental errors. They are

(i) Separation

Source and fiber input surfaces have the same axis, but they are separated by a gap s .

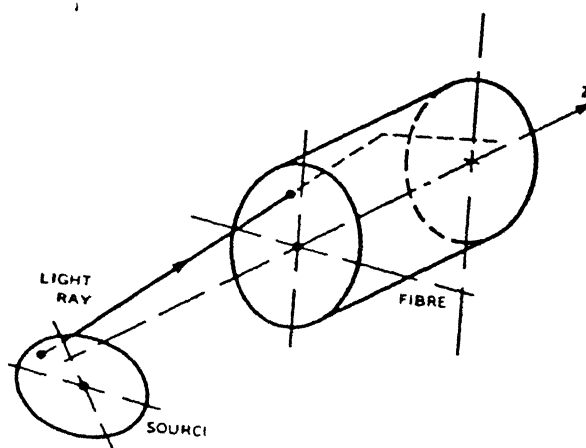
(ii) Lateral displacement

The axes of the two surfaces are parallel but separated by a distance d .

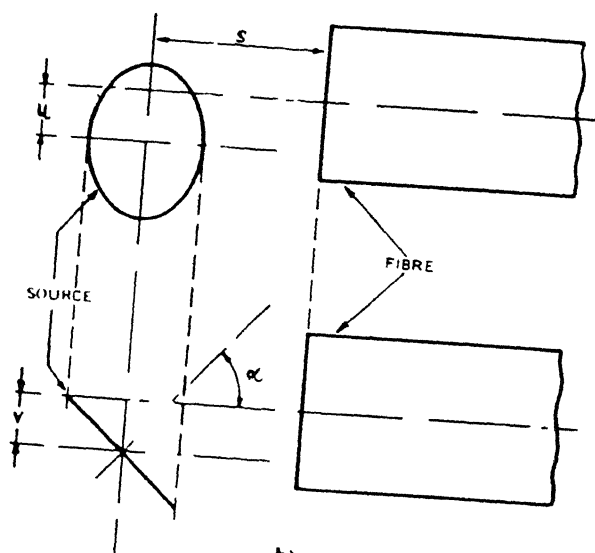
(iii) Angular misalignment

These two axes forming a certain angle α .

In practice, these three errors may be simultaneously present (fig 2.5). To minimize the coupling errors between the source and the fiber, a demountable connector, working on



a)



b)

FIG. 2 5
 Geometry of source-fiber coupling errors:
 (a) perspective view (b) orthogonal projection

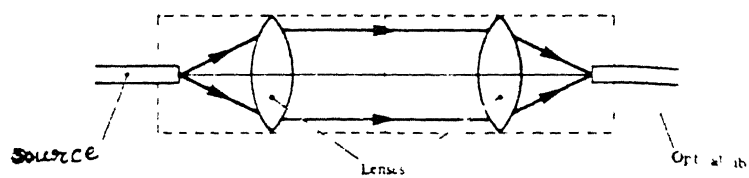


FIG 2 6
Expanded beam connector

the principle of expanded beam, is used. Fiber coupling with source utilizing this principle is shown in fig 2.6. As shown in this figure a connector consists of two lenses for collimating and refocusing the light from the source into the fiber. The use of this interposed optics makes the achievement of lateral alignment much more easy [8]. However, angular alignment remains difficult and a lot of skill is required for its reduction in a practical laboratory setup.

3.2 Propagation of higher order modes and attenuation consideration

With the advancement in the fiber optic technology, low loss fibers with a loss of 0.5 dB/Km at 850 nm are available. In case of single mode fibers, only one mode is excited and there is no mode to mode interference. However, higher order modes also propagate along with the dominant mode for small lengths of the fiber. Different modes of propagation are shown in fig. 2.7. The dominant mode is LP_{01} . The optical fibers in M-Z-I sensor are wound around a hollow copper cylinder to introduce microbends. As the attenuation increases due to microbending losses, the higher order modes i.e. LP_{11} , LP_{21} attenuate very fast and only the dominant mode LP_{01} propagates through the fiber. If higher order modes are present, the output beam gets

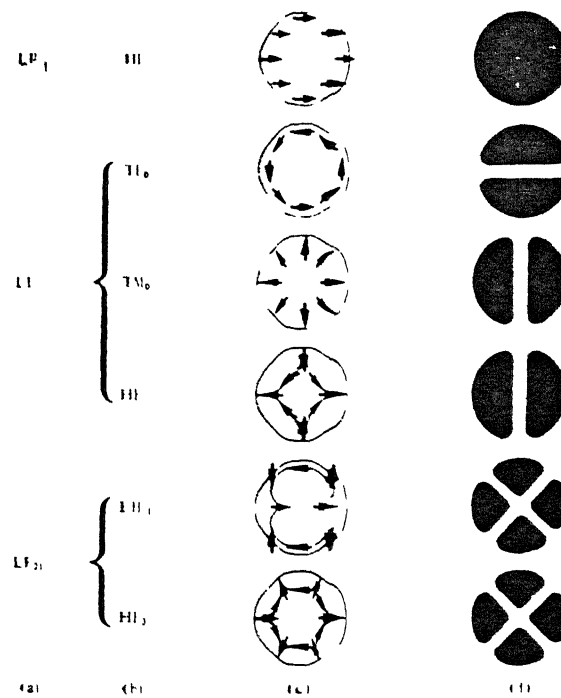


FIG 2.7 LP Modes - Propagation

- (a) LP mode designations,
- (b) exact mode designations,
- (c) Electric field distribution
- (d) Intensity distribution

distorted which affects the visibility of the fringe pattern [8].

2.3.3. Beam splitter microphonics

The position of the beam splitter critically affects the optical pathlength in both arms and this component must remain stationary within an accuracy of 0.1 nm. It is not expected that a 30 mm diameter plate will fulfil this requirement. Also the vibration of the beam splitter is a considerable source of random phase shifts. The noise observed is approximately 2×10^{-3} radians. The replacement of beam splitter with an all fiber 3dB single mode coupler reduce this noise by a factor of two [5]

2 3.4 Light source selection and associated problems

In principle, any light source which matches the specified fiber wavelength is suitable for use with a M-Z-I temperature sensor. However for satisfactory operation of M-Z-I, it is desirable for the light source to have a good coherence length, high collimation and good intensity. He-Ne gas lasers, as a light source, fulfil these properties very well. However, gas lasers are bulky and hence semiconductor diode lasers are considered for the M-Z-I. The advantages of diode lasers are

(1) small size,

- (ii) high efficiency,
- (iii) high output power,
- (iv) ease of modulation of light output.

Solid state GaAlAs single mode diode lasers make a convenient source for the fiber optic sensor system. However, changover from conventional gas laser sources (typically He-Ne lasers) to semiconductor sources leads to some additional problems as follows

- (i) Amplitude noise
- (ii) Phase noise
- (iii) Coherence length.

(i) Amplitude Noise

It has been observed that even small amounts of light feedback (approximately $10^{-3}\%$) into the laser cavity can cause the laser to jump to another longitudinal mode (but not always adjacent to the mode previously lasing). The phase and amplitude of the feedback under certain conditions cause the laser to oscillate between longitudinal modes. This has been shown to produce 20-60 dB of excess noise incurred which is very undesirable. It is therefore extremely important to suppress feedback induced mode jumping as the noise incurred is clearly

unacceptable. It is necessary to ensure that fiber ends are either cut at an angle or index matched to avoid reflections. The splices and couplers in the sensor system must also be of a high quality to avoid reflections which are sufficient to produce mode hopping noise [1].

(ii) Phase noise

The phase noise is caused due to instabilities in the wavelength of the laser source. If a He-Ne laser is used to power the interferometer phase noise has a negligible effect on the output of the interferometer owing to the laser's good frequency stability. Very low frequency ($<1\text{Hz}$) drifts may be observed which are due to macroscopic changes in the length of the laser's cavity. If however a diode laser as a source is used, the noise is observed to be much larger and increases linearly with path difference. To avoid excess noise, it is necessary to use sensors with small path differences. In a M-Z fiber optic interferometer, matching of pathlengths to within 1mm is possible [1].

(iii) Coherence length

The coherence length of a diode laser, though smaller than that of a gas laser is still quite large for the purpose of an M-Z-I system. However, in presence of optical feedback, line

broadening, satellite mode generation and multimode generation limit the difference of optical pathlengths of the two fibers inspite of high coherence length. Broadening and satellite mode generation require pathlengths to be matched to approximately 1 cm, whereas multi-longitudinal mode emission of the laser cavity requires pathlength matching to 0.1 mm to ensure good fringe visibility [1].

It is clear that coherence length problems with the diode laser are not serious in interferometer systems provided excessive values of optical feedback are not encountered. Hence, care in design is necessary to ensure that reflection is kept approximately below $10^{-2}\%$ [1].

2.3.5 Modal noise

Modal noise in the optical fiber is generated due to intermodal dispersion. Disturbances along the fiber such as vibrations, discontinuities, connectors, splices and couplings lead to large modal noise [9]. It can be observed on the screen as a fluctuation in the speckle pattern. Hence it is often termed as speckle noise. Large speckle noise was observed in the experimental setup. It leads to a large noise in the photodetector. Modal noise can be controlled by

- (i) proper optical alignment
- (ii) reduction in mechanical vibrations
- (iii) use of single mode fiber.

However it can not be eliminated completely.

2.3.6 Effect of other physical variables

While the optical fiber sensor may be designed to monitor one particular physical variable, e.g. temperature, the effect of all other physical variables is always present in the background. It could be vibrations, acoustic signals, magnetic fields and a host of other variables. All these perturbations leads to noise in the sensor system and degrade the performance. Care has to be taken to isolate the effect of unwanted perturbations on the system.

2.4 Detection system

The detection system is required to either count the fringe movement or compute the phase shift caused due to temperature changes. It must have a high sensitivity and low noise. For photodetection, one can use either p-i-n photodiode or an avalanche photodiode. The signal from the photodiode detector is fed to a low noise preamplifier before further signal processing as shown in fig. 2.8.

- (1) proper optical alignment
- (11) reduction in mechanical vibrations
- (111) use of single mode fiber

However it can not be eliminated completely.

2.3 6 Effect of other physical variables

While the optical fiber sensor may be designed to monitor one particular physical variable, e g temperature, the effect of all other physical variables is always present in the background. It could be vibrations, acoustic signals, magnetic fields and a host of other variables. All these perturbations leads to noise in the sensor system and degrade the performance. Care has to be taken to isolate the effect of unwanted perturbations on the system.

2.4 Detection system

The detection system is required to either count the fringe movement or compute the phase shift caused due to temperature changes. It must have a high sensitivity and low noise. For photodetection, one can use either p-i-n photodiode or an avalanche photodiode. The signal from the photodiode detector is fed to a low noise preamplifier before further signal processing as shown in fig 2.8

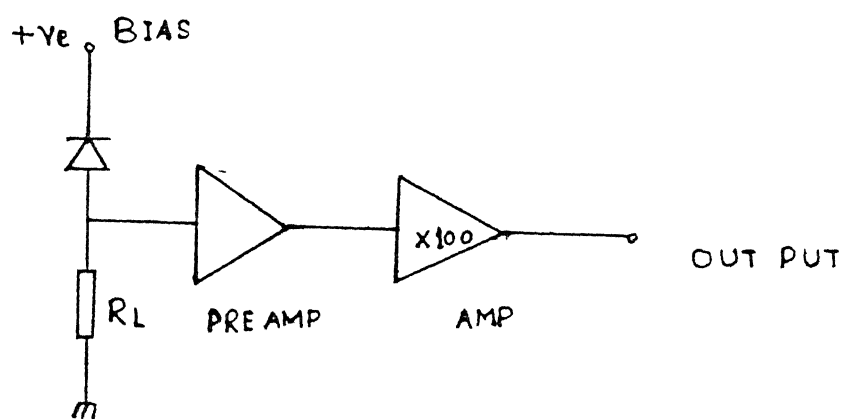


FIG 2 8

Detection system

2.4.1. Photodetector

The simplest fiber system detector is a pin photodiode. It is operated in a reverse biased mode. Noise generated in amplifier stages following the detector is a serious problem limiting the performance of detector. For a pin detector we get at most one electron per incident photon or about 0.5A/W of optical power emitted by the fiber. Since our interest is in detecting power levels of the order of 1 nW, it is desirable to have a mechanism to increase the detector responsivity beyond 0.5 A/W in order to overcome the thermal noise introduced by the preamplifier. The avalanche photodiode provides such a mechanism. The average responsivity of avalanche photodiodes can be 50 A/W or more. It is limited by the multiplication noise and by imperfections in the detector which cause premature breakdown at localized points in the detector [12].

The speed of response of a pin detector is governed by the time it takes for the carriers to cross the "intrinsic" region under the influence of the electric field. For APD detectors the speed of response is governed by the time it takes for the carriers to cross the "intrinsic" region plus the time required for the multiplication process in the high field region. Detectors of both types are presently available with the response time of less than 1ns. However, the speed of response is

not an important consideration since the rate of change of temperature generally is much lower than the response time of detector.

2.4.2. Preamplifier and amplifier

The photocurrent generated by the detector must be converted to a suitable signal for further processing with a high signal to noise ratio. The preamplifier is used as a first stage of amplification and thus its noise performance is critical. A FET preamplifier can be used to reduce the noise in the system. Later stages of the amplifier provide the remainder of the amplification of the signal. The load resistance R_L (fig. 2.8) is a main source of thermal noise and hence the value of R_L should be low. But the sensitivity of the detector also reduces with decreasing value of R_L .

CHAPTER - 3

SIGNAL RECOVERY TECHNIQUES FOR FIBER OPTIC INTERFEROMETRIC SENSORS

The purpose of the detection system is to transfer the optical output of the sensor into an electric signal proportional to the amplitude of the signal. The detection systems for interferometric sensors are more complex than those for amplitude sensors. In this chapter different detection schemes for interferometric sensors are reviewed.

3.1 Introduction

A generalized form of interferometer connected to a generalized detection system is as shown in fig. 3.1.

For simplicity the signal is considered to act only on the reference arm. The essential features of the various detection systems are discussed assuming analysis for linearly polarized light and that the fiber is polarization insensitive [1]. In this case the electric field in the signal arm just before the combiner can be represented as

$$E_s = E_s^0 \exp [i\omega t + s(t) + \phi_s] \quad (3.1)$$

The electric field at the corresponding point in the reference arm is:

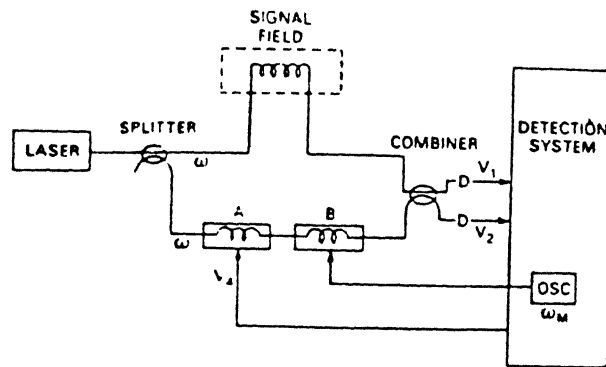


FIG 3 1

Generalized fiber interferometer
and detection system

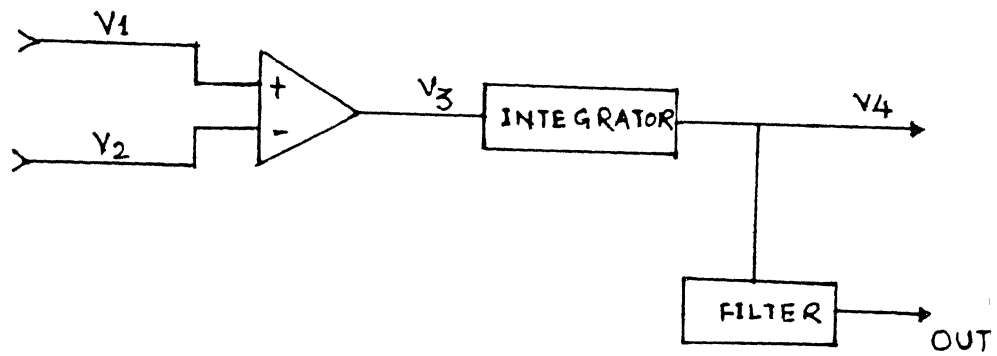


FIG 3 2

PTDC detection system

$$E_r = E_r^0 \exp [\omega_r t + A(t) + B(t) + \phi_r] \quad (3.)$$

In these expressions $s(t)$ is proportional to signal amplitude. Typically, $s(t) \ll \pi$. The arbitrary phase factors the signal and reference arms are ϕ_s and ϕ_r respectively. In an ideal case ϕ_s and ϕ_r would be constant. However, in fiber interferometers ϕ_s and ϕ_r drift in a quasi-random fashion. In a few seconds the drift in phase difference can easily be of the order of 2π or greater. Two modulator type terms [A and B] are included in the phase of the reference arm. These phase terms are generated by stretching sections of fiber wound on piezoelectric cylinders by applying electric signals to the piezoelectric elements. Depending on the type of detection system actually used, either A or B or none of these is present. The convention used in this discussion is that A represents phase produced by a feedback circuit to hold the interferometer at the quadrature condition. The phase B is always of the form $\phi_m \sin(\omega_m t)$. It is produced by driving the piezoelectric element with an oscillator.

The detection systems currently in use fall into five classes. These are

- (i) Passive homodyne (HDM)
- (ii) Homodyne with dc phase tracking (PTDC).
- (iii) Homodyne with ac phase tracking (PTAC).

(iv) True homodyne (HET)

(v) Synthetic heterodyne (SHET).

The configuration in terms of fig. 3.1 for each of these is given in table (I) [1]

Table - I

S.No.	Detection system	frequency	A	B
1.	HOM	$\omega = \omega'$	No	No
2.	PTDC	$\omega = \omega'$	Yes	No
3.	PTAC	$\omega = \omega'$	Yes	Yes
4.	HET	$\omega \neq \omega'$	No	No
5.	SHET	$\omega = \omega'$	No	Yes

3.1.1 Passive homodyne.

The most straight forward detection system is the passive homodyne (HOM). In this scheme a constant phase difference, $\phi_s - \phi_r = \pi/2$, is introduced between the reference and sensing arm. Simple interference of E_r and E_s in the balance optical mixer implemented by the combining coupler and the two photodiodes produce two electric signals V_1 and V_2

The operations of differentiation and multiplication would typically be implemented with analog circuits. The result is a linear combination of $s(t)$ and $\phi_s - \phi_r$. If the drift in ϕ_s and ϕ_r is in a different frequency band than $s(t)$, this drift can be filtered out from the output. One pays a price in the resulting complexity of the scheme in that the two output signals 90° apart need to be produced. A method for performing this function is by using a 3×3 coupler instead of a standard 2×2 coupler which reduces the complexity of the system. The performance limitation in HOM detection system is due to the distortion induced by the nonlinear processing. Also all real four quadrant analog multipliers have inaccuracies which corrupt the detected signal and limit the minimum detectable signal $s(t)$ [1].

3.1.2 Phase tracking homodyne detection systems (PTDC and PTAC)

The phase tracking homodyne detection system works on the principle of maintaining the quadrature condition at the output of the coupler by using a mechanical feedback. Usually this is achieved by applying feedback voltage to a piezoelectric stretching element which stretches the reference arm to produce a phase shift of A . As a consequence the error voltage is produced which is linearly proportional to the signal under quadrature condition.

The operation of the PTDC is the simpler of the two. In this case, the signal V_3 of equations (3.1) and (3.2) becomes

The operations of differentiation and multiplication would typically be implemented with analog circuits. The result is a linear combination of $s(t)$ and $\phi_s - \phi_r$. If the drift in ϕ_s and ϕ_r is in a different frequency band than $s(t)$, this drift can be filtered out from the output. One pays a price in the resulting complexity of the scheme in that the two output signals 90° apart need to be produced. A method for performing this function is by using a 3x3 coupler instead of a standard 2x2 coupler which reduces the complexity of the system. The performance limitation in HDM detection system is due to the distortion induced by the nonlinear processing. Also all real four quadrant analog multipliers have inaccuracies which corrupt the detected signal and limit the minimum detectable signal $s(t)$ [1].

3.1.2 Phase tracking homodyne detection systems (PTDC and PTAC)

The phase tracking homodyne detection system works on the principle of maintaining the quadrature condition at the output of the coupler by using a mechanical feedback. Usually this is achieved by applying feedback voltage to a piezoelectric stretching element which stretches the reference arm to produce a phase shift of A . As a consequence the error voltage is produced which is linearly proportional to the signal under quadrature condition.

The operation of the PTDC is the simpler of the two. In this case, the signal V_3 of equations (3.1) and (3.2) becomes

$$V_3 = 2V_0 \alpha \cos[s(t) + \phi_s - \phi_r - A] \quad (3.7)$$

Near the quadrature condition this becomes

$$V_3 = 2V_0 \alpha [s(t) + \phi_s - \phi_r - A - \pi/2] \quad (3.8)$$

$$\approx 2V_0 \alpha [\epsilon - A] \quad (3.9)$$

If an appropriate feedback voltage can be produced from V_3 and applied to a piezoelectric element, the phase A can be made to exactly cancel the error ϵ , thus driving the error signal to zero. Such a feedback signal is the integral of V_3 , given as

$$V_4 = g \int_0^{\tau} V_3(t') dt' \quad (3.10)$$

The complete form of this PTDC scheme is as shown in fig. 3.1 and fig. 3.2.

The differential equation for the feedback signal V_4 is

$$\frac{d}{dt} V_4 + gh 2V_0 \alpha V_4 = g\alpha 2V_0 \epsilon \quad (3.11)$$

where h is a constant dependent on the piezoelectric stretcher. The combination $gh2V_0\alpha$ is the gain bandwidth product of the feedback circuit. If the variation in $s(t)$ corresponds to frequencies much less than the gain bandwidth product, equation (3.11) ensures that $A = V_4 h = \epsilon$, which is the quadrature

condition. Since $hV_4 = \phi = s(t) + \phi_s - \phi_r - \pi/2$, V_4 is linear in the signal $s(t)$. Thus, $s(t)$ can be separated from ϕ_s and ϕ_r by an appropriate filtering [1].

The strong point of PTDC detection system is that it involves only linear operations. This is possible because the phase shift A produced by the piezoelectric element is a linear function of feedback voltage V_4 .

A drawback to PTDC scheme is that the voltage range of the integrator producing V_4 is limited in a practical system to $\pm 10V$. Once this voltage is approached, V_4 must be reset to zero. This reset produces a glitch in the output which must be appropriately smoothed out.

The PTAC scheme is a variant of the PTDC system. This system uses an oscillating phase term B as well as a feedback phase A . The oscillating phase causes the signals V_1 and V_2 to oscillate at frequency ω_m (approximately 100 KHz) and its harmonics. The oscillating signal V_3 is mixed with the local oscillator which drives the piezoelectric element B (refer fig 3.1). This mixing produces a slowly varying signal proportional to

$$\cos[s(t) + \phi_s - \phi_r - A] \quad (3.12)$$

This is of the same form as V_3 in the PTDC scheme. The rest of the feedback circuit is essentially identical to that of the PTDC.

The difference between the PTDC and PTAC scheme is that the PTDC scheme uses a low frequency signal V_3 directly as the error signal, while the PTAC scheme uses a high frequency signal as an error signal [1].

Relative to the PTDC scheme, the PTAC scheme has the disadvantage of greater complexity but better control of the gain bandwidth product.

3.1.3 Heterodyne detection system (HET)

The heterodyne detection system (HET) is one of the simplest in concept. Typically a Bragg cell (not shown in fig. 3.1) is used to shift the optical frequency of one arm of the interferometer with respect to the other. The output signal V_3 in this case is given by

$$V_3 = 2V_0 \alpha \cos[(\omega - \omega')t + s(t) + \phi_s - \phi_r] \quad (3.13)$$

Typically $(\omega' - \omega)$ is in the range of 100 KHz. Equation (3.12) is the classic form of a phase modulated carrier. There are a number of ways of extracting a signal linear in $s(t)$. Perhaps the simplest is to apply V_3 to the input of an FM discriminator tuned to $(\omega' - \omega)$. The output of FM discriminator is then

$$d/dt[s(t) + \phi_s - \phi_r] \quad (3.14)$$

The disadvantage of this scheme is the use of Bragg cell which is an undesirable bulk optic element consuming atleast a watt of electronic power and introducing alignment problems [1]

3 1.4 Synthetic heterodyne detection system (SHET)

The signal V_3 in this case is

$$V_3 = 2V_0 \alpha \cos[\phi_m \sin \omega_m t + s(t) + \phi_s - \phi_r] \quad (3.15)$$

Typically, ϕ_m is approximately 1, ω_m approximately 100 KHz. This signal which has components at ω_m , $2\omega_m$ etc., is the input to the circuit depicted in fig. 3.3. In brief, one branch of the circuit produces

$$V_T = \cos(3\omega_m t) \sin[s(t) + \phi_s - \phi_r] \quad (3.16)$$

and the other produces

$$V_B = \sin(3\omega_m t) \cos[s(t) + \phi_s - \phi_r] \quad (3.17)$$

In one case, $2\omega_m$ from the oscillator circuit combines with ω_m from V_3 to produce $3\omega_m$. In the other case, ω_m from the oscillator combines with $2\omega_m$ from V_3 to produce $3\omega_m$. Since the circuit operates at high frequency, 90° phase shifts are easy to obtain as required. The adder produces

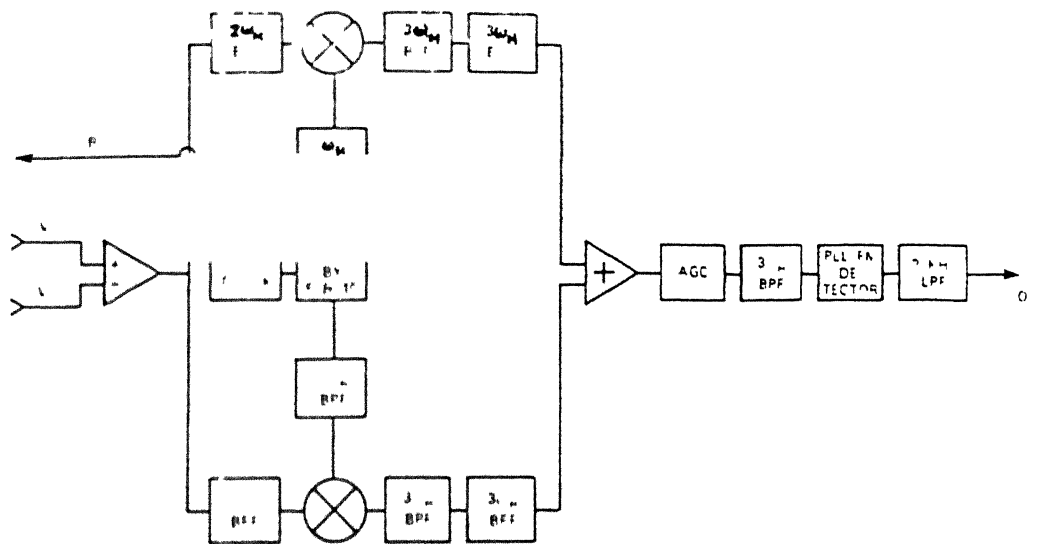


FIG 33

Synthetic heterodyne [SHET] detection system

$$V_H = V_B + V_T = \sin[3\omega_m + s(t) + \phi_s - \phi_r] \quad (3.18)$$

This signal has essentially the same form as that of the heterodyne signal of equation (3.13). Infact it is a heterodyne signal synthetically produced. The advantage of this method of producing the heterodyne signal is that, the bulk optics are not needed. Only a piezoelectric stretcher is required. A disadvantage of the synthetic approach is that drift in phase and mismatch in amplitude are introduced. These give rise to an output signal that is not a pure heterodyne signal. This will corrupt the output of the FM discriminator and limit the minimum detectable signal [1].

The final step in heterodyne detection systems is the extraction of $s(t)$ from a signal of the form equation 3.18. As mentioned earlier, the simplest approach is to use an FM discriminator tuned to ω_m .

3.2 Interferometric sensor detection system tradeoff

There is no single optimum detection system for all applications of fiber optic interferometric temperature sensors. Each scheme has advantages and disadvantages which need to be evaluated for a particular application. Table II gives the current understanding of the tradeoff analysis. [1].

Table - II

Cause	HOM	PTDC	PTAC	HET	SHET
Feedback to interferometer required	No	Yes	Yes	No	No
Special interferometer configuration required	Yes	No	No	Yes	No
Signal distortion characteristics	Fair	Good	Good	Good	Fair
Complexity of electronics	Medium	Low	Medium	Medium	High
Freedom from reset glitch	Yes	No	No	Yes	Yes
Freedom from oscillator phase noise	Yes	Yes	Yes	No	No
Laser amplitude noise rejection	Yes	Yes	No	No	No

CENTRAL LIBRARY
PAT. KANPUR
107:03
REC 210

CHAPTER - 4

EXPERIMENT AND RESULTS

4.1 Experiment

The fiber optic interferometer based on M-Z-I principle implemented (refer fig. 2.4) using a 1 mw He-Ne gas laser source ($\lambda=0.633\mu\text{m}$) and two lengths of single mode step index fiber. The laser output was divided by a cube beam splitter and resulting two beams coupled into the two fibers by a pair of microscope objectives, with N.A. = 0.25. The output ends of fibers were placed side by side with their axes parallel separated by one fiber diameter (approximately $100\mu\text{m}$), such that their expanding output beams overlap. Fiber pairs of 2m length each, were used with lengths matched to within 5 cm. The fibers were wound on copper cylinder with inner diameter 18 mm and outer diameter 20 mm. As the copper has high thermal coefficient of expansion variation in the length of the fiber with temperature is high giving higher sensitivity to the sensor. The sensor was placed in a water bath temperature of which could be changed. The overlapping output beams were observed on a screen where they formed parallel bright and dark interference fringes.

4.2 Detection scheme

A small pinhole [1 mm dia] was made on the screen to monitor the fringe pattern on a photo-detector. As the temperature of signal arm increases, fiber expands and the path difference increases. Hence the fringes move. This movement in the fringes was detected.

4.2.1 Circuit description

An APD detector is used for the detection of dark and bright fringes. The detector circuit is as shown in fig 4.1.

The transimpedance amplifier is used as I-V converter and the second stage is a gain stage. The sensitivity of the circuit depends on the value of resistance R_L . The typical values of R_L are in the range of 10Ω to $1\text{ M}\Omega$ (the one used in the circuit is $100\text{ K}\Omega$). With the increase in the value of R_L the thermal noise increases. Whenever dark and bright bands shift from the field of view, the comparator changes the state.

This output can be given to a counter which counts the number of fringes crossing the field of view per $^{\circ}\text{C}$ change.

4.3 Component specifications

(A) Optical Fiber:

SM .85-P fiber. Fujikura Ltd.

1. Single mode step index polarization preserving fiber.

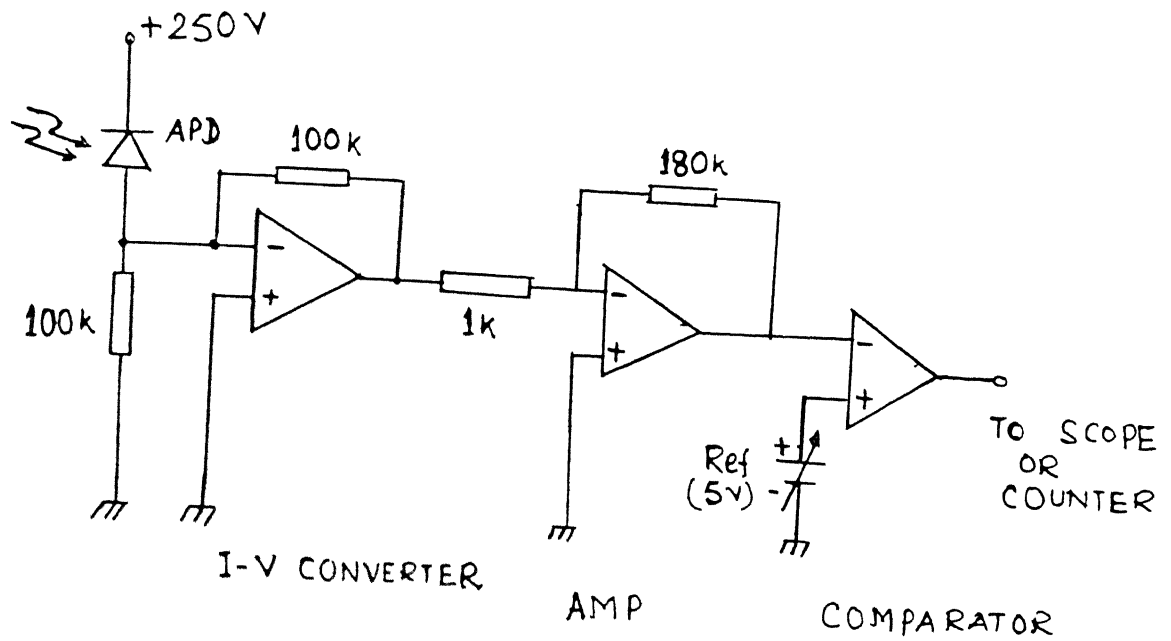


FIG 4.1
Photodetector circuit diagram

- ii. Wavelength: $0.85 \mu\text{m}$
- iii. Core diameter. $6 \mu\text{m}$
- iv. Cladding diameter $125 \mu\text{m}$
- v. Coupling length. 100-200 mm

(B) Cube-Beam Splitter:

- i. 03 BSD 044 MELLES GRIOT
- ii. Cubic: $A=B=C = 10 \text{ mm}$
- iii. Coating: All four faces multilayer HEBBAR
antireflection coating
- iv. Reflection and Transmission. $\approx 40\%$
- v. Wavelength: 650 to 900 nm.

(C) APD detector specifications

- i. RCA 30817
- ii. Breakdown voltage: 475 v
- iii. Responsivity: 17 Amp/watt
- iv. Operating voltage: 275 v
- v. Dark current: 142 nano Amp.
- vi. Noise current: $6.3 \times 10^{-13} \text{ Amp/Hz}^{1/2}$

(D) OP Amps:

RCA model : CA 081.

4 4 Results

A stationary fringe pattern which consists of dark and bright bands was observed on the screen for the M-Z-I temperature sensor as shown in fig. 4.2 The temperature of one of the arms of M-Z-I was increased. A rapid fringe movement was observed on the screen and also detected by an APD detector The output of the detector circuit was monitored on the oscilloscope Whenever a bright fringe crossed the detector surface a step in the output waveform was observed.

With an appropriate setup, the fringe ^{ve}moment can be calibrated to estimate the temperature change. However, in the M-Z-I arrangement fringe counting is difficult and there is no way of distinguishing between the upward and downward fringe movement. Hence only a rough estimate of the sensor temperature sensitivity could be made.

Fringe movement is also observed, whenever there is any source of vibration within a few feet of the experimental setup. It is necessary to control all sources of vibration to eliminate unwanted fringe movement. However this shows the high sensitivity of the sensor system to various perturbations.

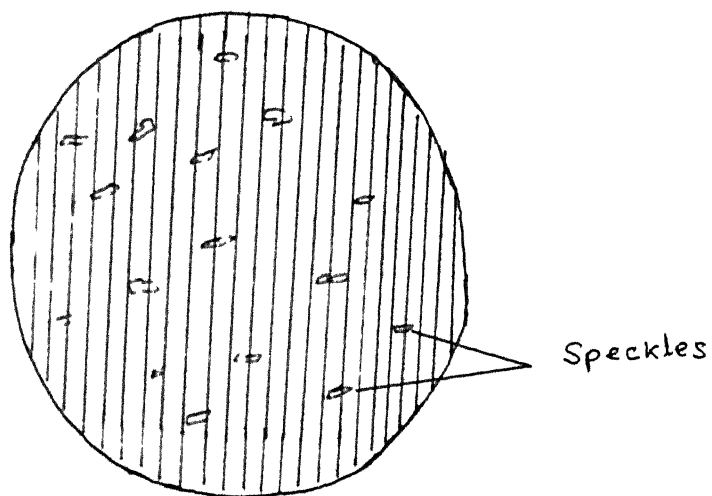


FIG 4 2
Interference pattern

CHAPTER - 5

DISCUSSION/MARKET AREAS AND CONCLUSION

5 1 Technologies

Interferometric devices for sensors are likely to show a gradual increase in use with time, with efforts initially remaining at the research level. Interferometric or polarization-dependent measurements for temperature sensing are unlikely to provide advantages for large volume markets other than for highly specific applications where the low thermal mass or sensor integration potentialities of the optical fiber are used. For such 'simple' measurements, the difficulties in maintenance etc. will also tend to be both technically as well as economically prohibitive for some time.

High technology developments will continue and fig. 5.1 is a simplistic component illustration of likely trends from the bulk optic interferometric device to the eventual incorporation of integrated optics and optical signal processing. Specialized primary and secondary coating work for optical fibers will be necessary to enhance sensitivities for specific requirements [2].

time scale

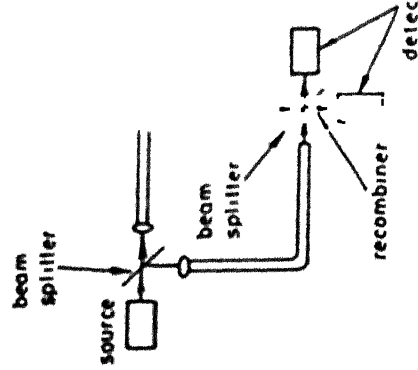
bulk optic-fibre
interferometer
1978-1981

all fibre
interferometer
1981-

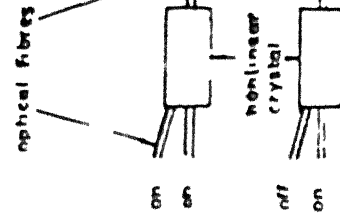
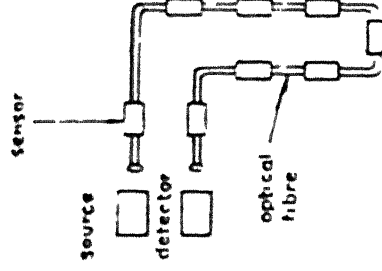
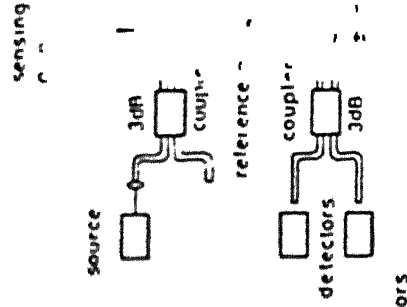
integrated optics
1980

coherent extended
sensors
1986 -

optical signal
processing
1990 -



schematic



integrated 2x2 3dB coupler

technology used

half-silvered beam
splitters
optical bench

fibre components
e.g. 2x2 1dB couplers
3x3 5dB couplers
semiconductor laser

diffused regions in crystal
to form
e.g. 3dB coupler
interferometer phase
compensation active
and passive devices

coherent detection
techniques

nonlinear optical
in crystals produce
AND/OR etc gate
switching

features

flexible but cumbersome
sensitive to noise
large volume

lower inherent noise
compatible with fibre-
optic links
sensor head may be
remote
smaller volume

difficult and slow
technology
problems with source and
detector interface
robust and small

many sensors may be
multiplexed onto one
fibre
remote interrogation

speed of light sensing
processing
reduced size and
weight
be placed near sensor
head

Fig 5.1 Technology trend in optical fiber sensors. [2].

5 1.1 Market Areas

Table III shows the several examples of the optical fiber sensors market areas [1]

Table III

Area	Methods (Examples)	Comments
Medical	Analytical; surface absorption; eg. anti body antigen immobisation. Total internal reflection. Laser doppler	Throwaway Small devices for insertion blood flow etc.
Defence	Surveillance, acoustic, magnetic, magnetic navigation, IIG, Fire, flush, radiation, temperature, fail safe switches etc.	All types required from extended to point sensors
Aerospace	Encoders, switches, pressure, displacement machinery condition monitoring	Should have low weight and withstand shock, vibration and large temp. range.
Utilities	Gas detection, point and over an area, transformer temperatures etc.	Specialized applications.
Industries	Flow, pressure, temperature etc. combustion energy control.	Should be cost competitive and will require multiplexing.

5.2 Conclusions

A single mode fiber optic M-Z interferometer is developed to demonstrate the temperature changes in one of the fiber arms. The sensitivity of such an interferometric sensor for temperature measurement is high.

In order to detect the increase or decrease in the temperature, the fringe movement in either direction can be monitored by using photodetector array or a CCD camera.

The disadvantages of this technique include the alignment requirements for the interferometer, the need to observe the motion of optical fringes and the fact that the measurement is of the change in average temperature of one fiber arm with respect to the other. Use of long fiber can provide adequate sensitivity. The fiber can either be coiled in a dimension less than an acoustic wavelength to provide a point sensor or it may be laid out over many acoustic wavelengths to provide a directional antenna. Detection of the phase modulated signal may still remain a problem, but possible solutions exist, as reviewed in chapter 3.

REFERENCES

- (1) THOMAS G. GIALLORENZI, et. al.
"OPTICAL FIBER TECHNOLOGY"
IEEE Journal of Quantum Electronics, Vol Q.E. 18, No. 4
April 1982, pp. 626-665.
- (2) G.D. PITT, et.al.
"OPTICAL FIBER SENSORS"
IEE Proceedings, Vol. 132, Pt. J , No 4, August 1985
pp.214-245.
- (3) N. LAGOKOS, J.A. BUCARO, and J. JARZYNSKI
"TEMPERATURE-INDUCED OPTICAL PHASE SHIFTS IN FIBERS"
Applied Optics/1 July 1981/Vol. 20, No 13, pp. 2305-2308.
- (4) G.B. HOCKER
"FIBER-OPTIC SENSING OF PRESSURE AND TEMPERATURE"
Applied optics/1 May 1979/Vol. 18, No. 9, pp. 1445-1448.
- (5) IEE, FIRST INTERNATIONAL CONFERENCE ON
"OPTICAL FIBER SENSORS"
London, (26-28) April 1983.
- (6) All India Symposium on
"FIBER OPTIC SENSORS"
(Organized under the IISC-ISRO Educational Programme)
March 18-19, 1983, Indian Institute of Science, Bangalore.

- (7) Journal of the Institution of Electronics and Telecommunication Engineers.
Vol. 32, No. 4, July-August 1986. Special Issue on Optoelectronics and optical communications.
- (8) JOHN SENIOR
"OPTICAL FIBER COMMUNICATIONS PRINCIPLES AND PRACTICE"
Prentice-Hall International series in Optoelectronics.
Series editor: P.J. Dean. 1985
- (9) "OPTICAL FIBER COMMUNICATION"
Technical Staff of CSELT Torino(Turin) Italy.
McGraw-Hill Book Company.
- (10) "PRINCIPLES OF OPTICS"
Born & Wolf - 4th Edition.
Peragamon Press 1970 Ch. 2.
- (11) "OPTICAL FIBER TECHNOLOGY", II
(IEEE Press Selected Reprint Series)
Edited by Charles K. Kao Chief Scientist
Electro-optical products division, International Telephone and Telegraph Corporation, IEEE Press
The Institute of Electrical & Electronics Engineers, Inc. New York.

(12) H. KRESSEL

Topics in applied physics, Vol. 39

"SEMICONDUCTOR DEVICES"

for optical communication,

Second updated edition, Springer-Verlag, Berlin,

Heidelberg, New York.

(13) A. BRUCE BUCKMAN

"ANALYSIS OF A NOVEL OPTICAL FIBER INTERFEROMETER WITH
COMMON MODE COMPENSATION"

J. of light wave technology, Vol. 17, No. 1, Jan. 1980,
pp. 151

(14) HECHT OPTICS (Second Edition)

Eugene Hecht., Adelphi University, Addison-Wesley
publishing Co., pp. 592-593.

EE-1990-M-GAT-INT